Graphene field-effect transistor application for flow sensing

Maciej Łuszczek[1,*], *Dariusz* Świsulski[1], *Robert* Hanus[2], *Marcin* Zych[3], and *Leszek* Petryka[4]

[1]Gdańsk University of Technology, Faculty of Electrical and Control Engineering, 80-233 Gdańsk, Poland
[2]Rzeszów University of Technology, Faculty of Electrical and Computer Engineering, 35-959 Rzeszów, Poland
[3]AGH University of Science and Technology, Faculty of Geology, Geophysics and Environmental Protection, 30-059 Kraków, Poland
[4]AGH University of Science and Technology, Faculty of Physics and Applied Computer Science, 30-059 Kraków, Poland

Abstract. Microflow sensors offer great potential for applications in microfluidics and lab-on-a-chip systems. However, thermal-based sensors, which are commonly used in modern flow sensing technology, are mainly made of materials with positive temperature coefficients (PTC) and suffer from a self-heating effect and slow response time. Therefore, the design of novel devices and careful selection of materials are required to improve the overall flow sensor performance. In this work we propose graphene field-effect transistor (GFET) to be used as microflow sensor. Temperature distribution in graphene channel was simulated and the analysis of heat convection was performed to establish the relation between the fluidic flow velocity and the temperature gradient. It was shown that the negative temperature coefficient (NTC) of graphene could enable the self-protection of the device and should minimize sensing error from current-induced heating. It was also argued that the planar design of the GFET sensor makes it suitable for the real application due to supposed mechanical stability of such a construction.

1 Introduction

There is a number of potential applications for micro sensors, e.g. for monitoring of gas or fluid flow including flow cytometry, cleanroom environmental monitoring, wind, gas chromatography, viscosity measurements and so on (see e.g. Ref. [1] for the review). These sensors complement technologies such as microfluidic channels, valves, pumps, and heaters that are assembled together in the so-called lab on a chip devices or micro total analysis systems.

Thermal-based flow sensors usually utilize the hot-wire configuration. The sensing principle of such a device is based on the dependence of the sensor heat transfer on the fluid velocity, temperature and composition. The conventional hot-wire sensor consists of a thin metal wire or a film made of a material with a high temperature coefficient of resistance such as tungsten, platinum, platinum-rhodium and platinum-iridium. At the first approximation, when the wire is heated by an electrical current I, the thermal energy generated by the wire equals the energy loss due to convective heat transfer at the equilibrium state, $I^2R_w = A_w (T_w - T_f)h$, where A_w denotes the surface of the wire, T_w and T_f are the wire and fluid temperatures, respectively, h is the heat transfer coefficient and I^2R_w represents Joule heat. The resistance of the hot wire (R_w), naturally, depends on the wire temperature (T_w). At the steady state, this resistance can be expressed using a linear approximation of the wire temperature, $R_w = R_0 [(1+ \alpha (T_w - T_f)]$, where R_0 is the baseline resistance of the wire and α is the TCR. The heat transfer coefficient (h) can be expressed as the function of fluid velocity (V_f) according to King's law, $h = a + bV_f c$, where a, b and c are the constants obtained from experimental calibrations. Finally, the fluid velocity V_f can be evaluated from the above-mentioned equations. It is worth to note at this place, that the sensitivity of the device to the flow velocity is provided by having the wire or film temperature T_w substantially higher than the fluid temperature T_f. Additionally, the measurement of voltage drop across the wire allow also to determine local fluid velocity, if only the physical properties of the gauge material and the mechanism of heat transfer are well known. Generally, the hot-wire devices operates in two regimes, that is, (1) a constant-current regime (I_w = const) when the gauge voltage pulsations are attributable to temperature variation and, hence, the wire resistance, and (2) the regime of constant temperature (T_w = const), maintained by the feedback system with a variable current heating the sensor. One or the other regime is used depending on the specific character of the measurements. However, the hot-wire sensors, which are commonly used in modern flow sensing technology, exhibit some essential limitations, because they are mainly made of materials with positive temperature coefficients (PTC) and suffer from a self-heating effect and slow response time. Therefore, the design of novel devices and careful selection of materials are required to improve the overall flow sensor performance.

Graphene is considered as an interesting new material in this context. It is a two-dimensional honeycomb crystal made of carbon atoms, exhibiting electrical mobility and thermal conductivity over an

* Corresponding author: maciej.luszczek@pg.gda,pl

order of magnitude greater than silicon. The electronic properties of graphene layer can be easily tuned with the use of an external gate. The variation of the gate (G) voltage with respect to source (S) or drain (D) terminals influence electron and hole densities and as a result we obtain an ambipolar graphene field effect transistor (GFET). The principle of its operation is the same as in the case of the conventional metal-oxide semiconductor field-effect transistor (MOSFET), that is, it is based on the so-called field effect which enables to control the conductivity in the graphene channel region by an electric field generated by the applied external voltage. More precisely, the shape of the channel and the flow of the charge carriers from the source to the drain is influenced by the voltage applied across the insulated gate and the source. Electronic structure of graphene indicates that it is a zero-gap semiconductor with characteristic linear dispersion near the Fermi level. The type of carriers and the carrier density in the channel depend on the potential difference between the channel and the gate. As a consequence, the two branches of the transfer characteristics, separated by the charge neutrality point (so-called Dirac point), are visible. At the Dirac point the minimum conductivity and maximum resistance are observed [2]. This material has a large surface-to-volume ratio, low thermal inertia and high sensitivity to temperature variation. What is more, the negative temperature coefficient (NTC) of graphene should enable the self-protection of the sensors and the minimization of the sensing errors caused by the current-induced heating. Recently, it has been demonstrated that the graphene-based ”hot wire” device could be used as a nanoscale flow and temperature sensor [3].

In this work we propose graphene field-effect transistor (GFET) to be used as microflow sensor. Theoretical prediction of behavior of the newly designed graphene sensor is an essential task because the realization of the prototype seems to be costly and difficult due to many technological problems. It is why the simulation was performed at the first stage of the investigation. Here, we present the results of the preliminary study of the GFET device for the flow sensing application.

2 Computational method

We performed the calculations with the use of the GFET Tool program [4] which enables simulation of the electrical characteristics of a top-gated graphene field-effect transistor. The drift-diffusion approach was employed to calculate self-consistently *I-V* characteristics at different initial temperatures. Also the carrier density in the channel could be evaluated in this program. The velocity saturation, "puddle" charge density distribution, caused by different impurities and thermally excited carriers, Seebeck effect and device breakdown due to thermal self-heating are taken into account in the code, too. It is possible to examine the GFET device with various channel geometry W x L (W - width, L - length) different thicknesses of the top-gate dielectric and SiO_2 layers and various values of mobility of the both type of carriers (electrons and holes) could be set up. Also Dirac voltage can be declared at the beginning of the calculation.

In our study we simulated the GFET devices with W and L parameters from the range of 0.5 - 10 μm, the top-gate dielectric thickness of 10 nm and the 300 nm SiO_2 layer. The initial temperatures were from 300K to 400K. The mobility of carriers was assumed to be 3000 cm^2/Vs. Generally, we simulated the performance of the devices at the Dirac voltage of 0 V.

3 Results and discussion

Output characteristics (not presented here), $I_D(U_{DS})$, of all the modelled GFET with different graphene channel geometry, are similar to those of typical FETs. Either linear or saturation regions are noticeable at various initial temperatures, especially for gate-source voltages, U_{GS}, much higher than the Dirac voltage, U_{Dirac}. The drain saturation current depends directly on U_{GS}, what is typical for all types of FETs. There are some differences, however, in transfer characteristic, $I_D(U_{GS})$, when compared with the typical MOSFET. The threshold voltage is not observed, so the GFET is in a conduction state for all U_{GS} [5]. The drain current, I_D, reaches the minimum for U_{GS} close to the Dirac point voltage. One can also see a shift of the point of the minimal conductance towards positive values with increasing drain voltage U_{DS}. This effect can be explained by the influence of U_{DS} on the channel potential [6]. Maximum of channel resistance, R_m, corresponding to the minimum of the conductivity, is visible for U_{GS} close to Dirac voltage and it is in order of kΩ. The values of drain-to-source resistance, R, depend on U_{DS} voltage and the smallest values of the resistance are in the linear region of the output characteristics. All the obtained characteristics are in agreement with the previous simulations [2].

In Fig. 1 channel resistance vs. graphene dimensions with L x W up to 10 μm x 10 μm is shown. As is easy to notice, the resistance increase with L and decrease with W.

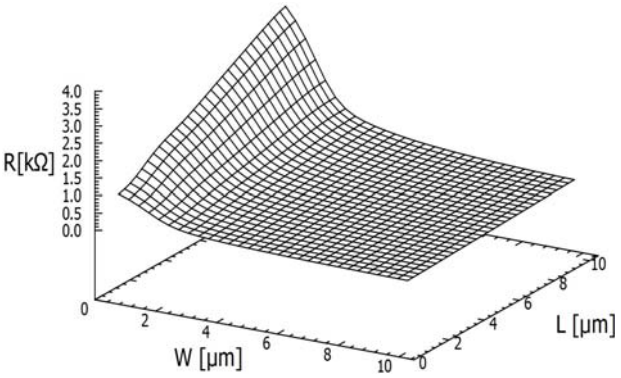

Fig. 1. Resistance vs. channel dimensions at room temperature (U_{DS} = 0.1 V, U_{GS} = 5 V, V_{Dirac} = 0 V).

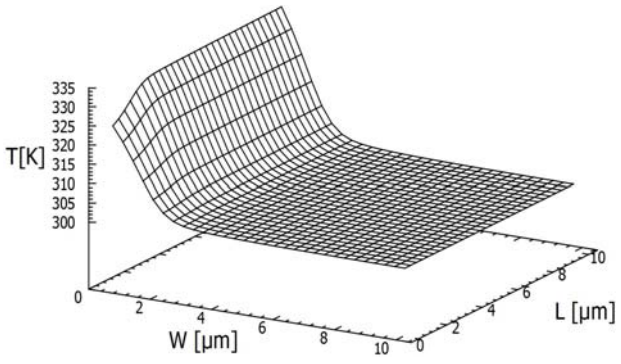

Fig. 2. Channel temperature vs. device dimensions (T_{ini} = 300K, U_{GS} = 5 V, U_{Dirac} = 0 V, I_{Dmax} = 0.5 mA).

Obviously, an electrical drain current is responsible for heating of the device and this effect depends strongly on the geometry of graphene sheet as it is presented in Fig. 2 for the case of GFET device at initial temperature of T_{ini} = 300K. The temperature of narrow (small W) and long (large L) graphen stripe rises significantly even for relatively low currents. To avoid self-heating one should design GFET with large W and small L, instead. On the other hand, this effect could be utylized when the graphene channel works as a "hot-wire" element for microflow sensing. The general idea of the device operation is as follows. The GFET element device should be heated by the drain current, I_D, and subjected to fluid flow. Electrical resistance, R, is supposed to change according to the channel temperature T. Thus, heat transfer rate can be transduced into a signal that depends on the fluid flow rate. Indeed, our simulations indicate that the resistivity of GFET device is temperature-dependent (Fig. 3). At the first approximation, the R-T dependence could be treated as a linear one for temperatures from the range of 300-400K. Our calculations also confirm the negative temperature coefficient (NTC) of graphene with the estimated value of $\alpha = -8.7 \cdot 10^{-4}$ K^{-1} for L x W = 3 μm x 10 μm. In the next stage, the as-prepared GFET-based device should be characterized by imposing a known fluid flow with stable temperature to calibrate the sensor by measuring the resulting resistance or voltage change. The fluids used to characterize the sensor should be the same as fluids which are planned to be measured since the thermal conductive properties of the fluid are integral to the transduction mechanism.

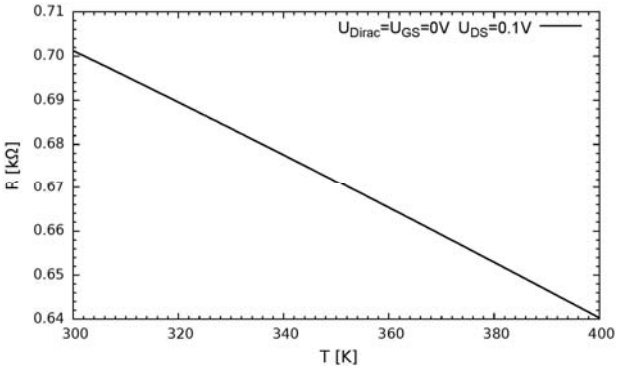

Fig. 3. Channel resistance vs. temperature (L = 3 μm, W = 10 μm, I_D = 0.5 mA).

Reported in the literature temperature maps of graphene field-effect transistors with distinct "hot spots" that appear along the channel and vary with the applied voltage imply that the primary heating mechanism is due to energy loss of carriers within the graphene channel and not due to contact resistance [7]. The GFET device goes from hole to electron-hole and electron conduction when the gate voltage changes, what is also reflected in the temperature profiles along the channel. Our calculations confirm that temperature hot spots are always located at the position of minimum carrier density (which is the "crossing point" of electron and hole concentrations – not presented here) along the graphene channel. The temperature profiles for different drain currents are collected in Fig. 4. As can be seen, the temperature and its distribution could be easily controlled by the drain current, I_D. (Note that GFET is heated to temperatures above 450K by 7 mA and 9 mA drain currents, what probably should lead to the breakdown of the real element.) Additionally, the location of the maximum could be changed by the gate voltage, U_{GS}.

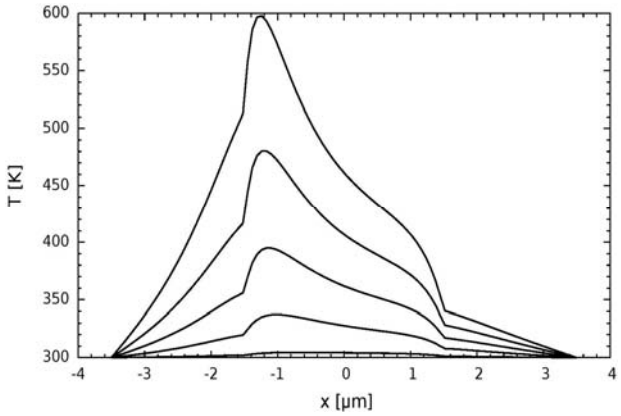

Fig. 4. Temperature vs. position along L direction in the channel (L = 3 μm, W = 10 μm, I_D = 0.5, 3, 5, 7, 9 mA, U_{Dirac} = U_{GS} = 0 V, T_{ini} = 300K).

4 Conclusions

Microflow sensors offer great potential for various applications, especially in microfluidics and lab-on-a-chip systems. However, thermal-based sensors, which are commonly used in modern flow sensing technology, are mainly made of materials with positive temperature coefficients and suffer from a self-heating effect and slow response time. Therefore, the design of novel devices and careful selection of materials are required to improve the overall flow sensor performance. Here, we propose graphene field-effect transistor (GFET) to be used as microflow sensor. Before concluding, it is relevant to summarize our findings. In this study the results of the simulation of a top-gated graphene field-effect transistor (GFET) were presented. We succeeded in reproducing typical GFET characteristics. Temperature distribution in graphene channel was simulated and it was demonstrated that the temperature of graphen channel, which could be treated as a "hot wire" for microflow sensing, can be controlled with the

choice of voltages applied on the three terminals. The negative temperature coefficient (NTC) of graphene was confirmed in our simulations, too, what could enable the self-protection of the device and should minimize sensing error from current-induced heating.

To evaluate flow sensitivities, the prototype of graphene "hot wire" GFET sensor should be placed in a kind of package with capillaries as upstream and downstream flow interconnections. During the measurement, the temperature of the analyzed fluid should be stabilized (e.g. at room temperature). The flow sensing responses of the GFET devices could be studied by monitoring the current and resistance changes of the graphene channel (for instance in the Wheatstone bridge configuration). In our opinion, GFET devices could be successfully employed for the flow sensing application due to their simplicity of design, ease of mass production in high-density array and potential mechanical stability of the planar construction. In the future the measurements of the real GFET-based sensors are planned what will allow for the direct comparison between the simulation and the experimental data.

References

1. J.T.W. Kuo, L. Yu, E. Meng, Micromachines, **3** (3), 550-573 (2012)
2. M. Łuszczek, M. Turzyński, D. Świsulski, Przegląd Elektrotechniczny, **91** (10), 170-172 (2015)
3. H. Al-Mumen, F. Rao, L. Dong, W. Li, Micro and Nano Letters, **8**, 681–685 (2013)
4. E. Pop, F. Lian, GFET Tool, DOI:10.4231/D3QF8 JK5T, https://nanohub.org/resources/gfettool, (2014)
5. F. Schwierz, Nature Nanotechnology, **5**, 487–496 (2010)
6. S. Rodriguez, S. Vaziri, M. Ostling, A. Rusu, E. Alarcon, M.C. Lemme, ECS Solid State Lett., **5** (1), Q39–Q41 (2012)
7. M.-H. Bae, Z.-Y. Ong, D. Estrada, E. Pop, Nano Lett., **10**, 4787–4793 (2010)